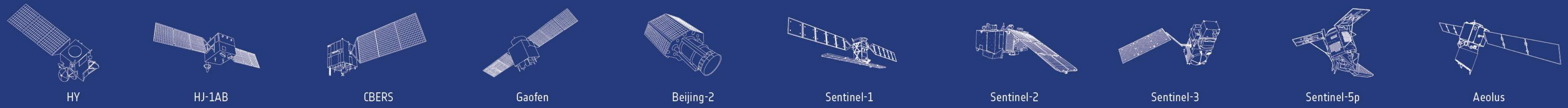

2023 DRAGON 5 SYMPOSIUM

3rd YEAR RESULTS REPORTING

11-15 SEPTEMBER 2023

[PROJECT ID. 58573]
THREE DIMENSIONAL CLOUD EFFECTS ON ATMOSPHERIC COMPOSITION AND AEROSOLS FROM NEW GENERATION SATELLITE OBSERVATIONS (3D CLOUD EFFECTS)

WEDNESDAY 13 SEPTEMBER 2023

ID. 58573

PROJECT TITLE: THREE DIMENSIONAL CLOUD EFFECTS ON ATMOSPHERIC COMPOSITION AND AEROSOLS FROM NEW GENERATION SATELLITE OBSERVATIONS (3D CLOUD EFFECTS)

PRINCIPAL INVESTIGATORS: PING WANG[1], MINZHENG DUAN[2]

CO-AUTHORS: Victor Trees[1], Benjamin Leune[1], Congcong Qiao[2]

PRESENTED BY: PING WANG

Dragon 5 3rd Year Results Reporting

- Inform on the project's objectives
- Detail the Copernicus Sentinels, ESA, Chinese and ESA Third Party Mission data utilised after 3 years (complete slide 4)
- Inform on the results after 3 years of activity
- Inform on the project's schedule, planning & contribution of the partners for the following year
- Report on the peer reviewed publications (nr. of papers, journal name and publication title) after 3 years of activity

Project's objectives

Detect the cloud shadows and

Analyze the impact of the 3D cloud effects on trace gas retrievals.

Use the (cloud) shadow and neighbour pixels to derive aerosol optical thickness and surface albedo.

Use 3D radiative transfer model simulations to understand the cloud effects on TROPOMI NO_2 products.

EO Data Delivery

Data access (list all missions and issues if any). NB. in the tables please insert cumulative figures (since July 2020) for no. of scenes of high bit rate data (e.g. S1 100 scenes). If data delivery is low bit rate by ftp, insert "ftp"

ESA /Copernicus Missions	No. Scenes
1. Sentinel-5P L1B, L2 (NO2, AAI, clouds)	8 months full orbits data
2.	
3.	
4.	
5.	
6.	
Total:	

Issues: No

ESA Third Party Missions	No. Scenes
1. Landsat-8	16
2.	
3.	
4.	
5.	
6.	
Total:	

Issues: No

Chinese EO data	No. Scenes
1.GF-2	30
2.	
3.	
4.	
5.	
6.	
Total:	

Issues: No

Results: cloud shadow detection: example in Europe

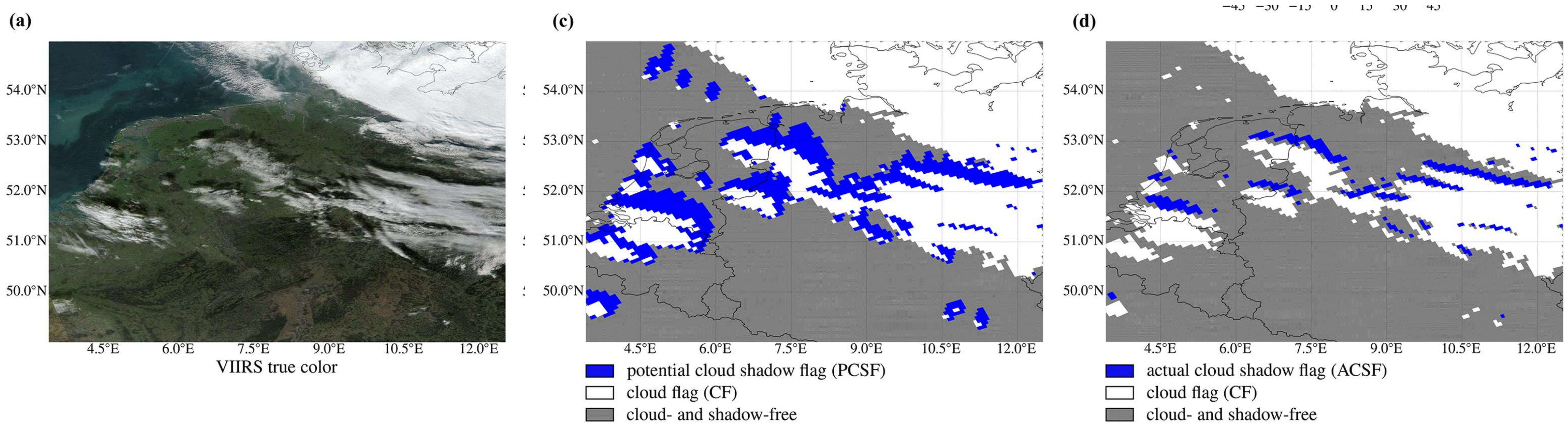

Trees et al., 2022

- Processed 8 months of TROPOMI data for cloud shadow flags
- Cloud shadow flags have been used to reprocess the TROPOMI DLER product

Results: impacts of shadows on NO_2 retrievals: principle

Steps to retrieve NO_2 VCD

- – fit slant columns (Ns)
- – separate Tropspheric and stratospheric columns (Ns_trop)
- – calculate airmass factors (AMF)
- – calculate vertical column

- Nv_trop = Ns_trop/AMF_trop

Small AMF leads to large NO_2 VCD

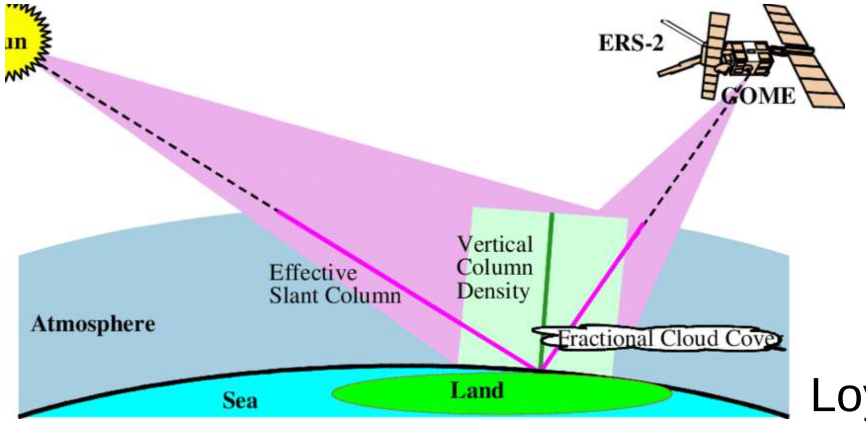

Loyola et al., 1996

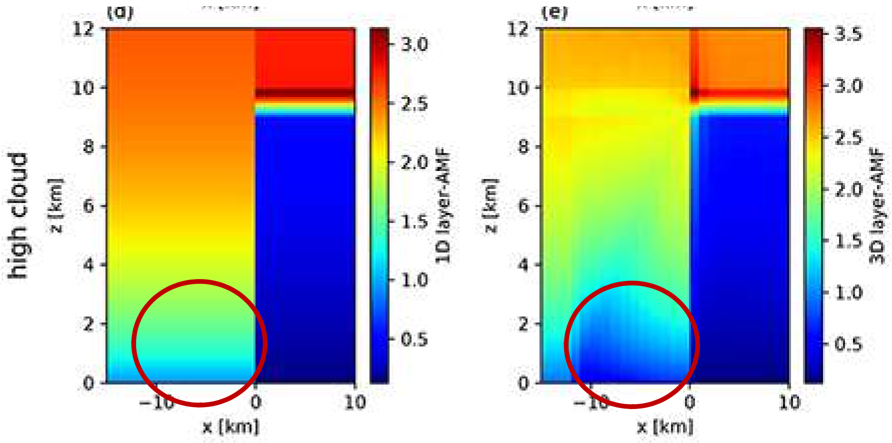

1D AMF 3D AMF

Figures taken from Emde et al., 2022 AMT

1D NO_2 AMF is larger than 3D AMF in the shadows. TROPOMI uses 1D AMF, retrieved NO_2 VCD in the shadow should be lower than the real NO_2 VCD.

But Yu, Emde et al., 2022 did not find lower NO_2 in the shadows in TROPOMI NO_2 data.

No cloud shadow signature found in TROPOMI NO_2

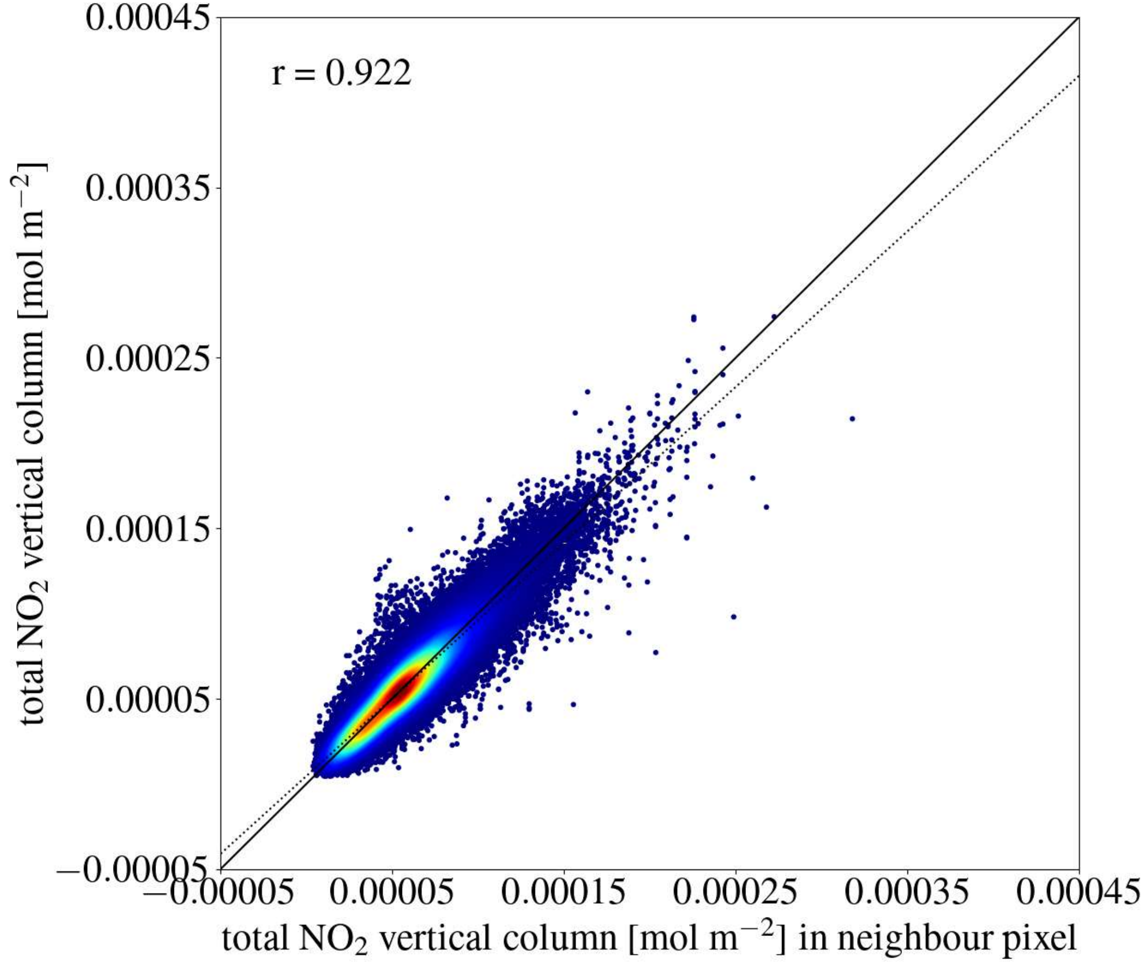

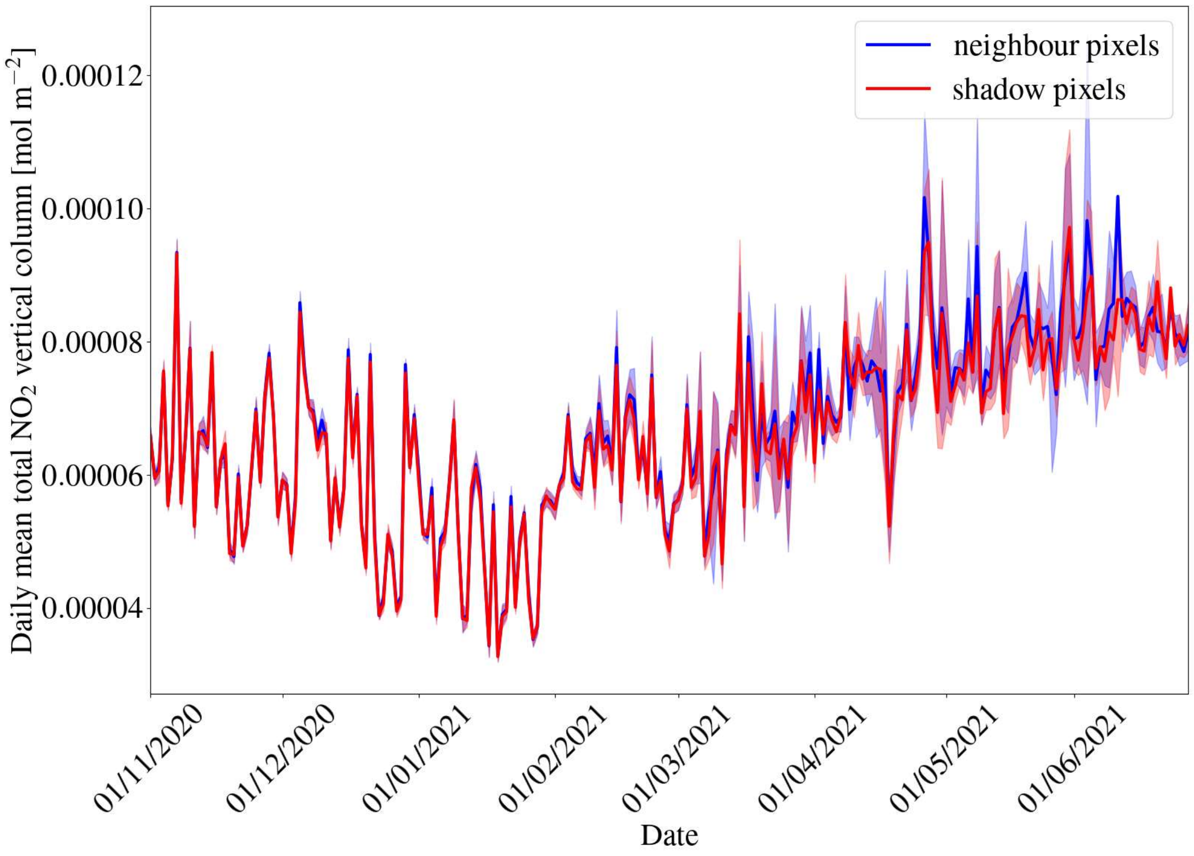

How to understand it?

MONKI (MONte carlo KnmI)

We have our own 3D RT model MONKI

```
PROGRAM main

  !***********************************************************************
  !*   MONKI (Monte Carlo KNMI) -- Version 1.0
  !*
  !*   Three-dimensional radiative transfer simulation of sunlight
  !*   reflected by an atmosphere-surface system following the Monte
  !*   Carlo technique, fully taking into account the state of
  !*   polarization of the light (Stokes parameters I, Q, U and V) for
  !*   all orders of scattering.
  !*
  !*   Atmosphere: - Rayleigh scattering of light by gaseous molecules
  !*               - Mie scatterring of light by spherical droplets
  !*               - Absorption of light by various gases (O3)
  !*               - Absorption of light by spherical droplets
  !*
  !*   Surface:    - Lambertian (reflecting the light isotropically
  !*                 and fully depolarizing) with specified surface
  !*                 albedo.
  !*
  !*   Domain:     - Cartesian grid
  !*               - Cyclic domain in horizontal (x- and y-)directions
  !*               - nx grid cells in the x-direction
  !*               - ny grid cells in the y-direction
  !*               - nz+1 grid cells in the z-direction
  !*
  !*   Author: Victor Trees, January 2023
  !*
  !***********************************************************************
```

MC code setup

- Rayleigh scattering
- O_3 absorption
- Surface reflection

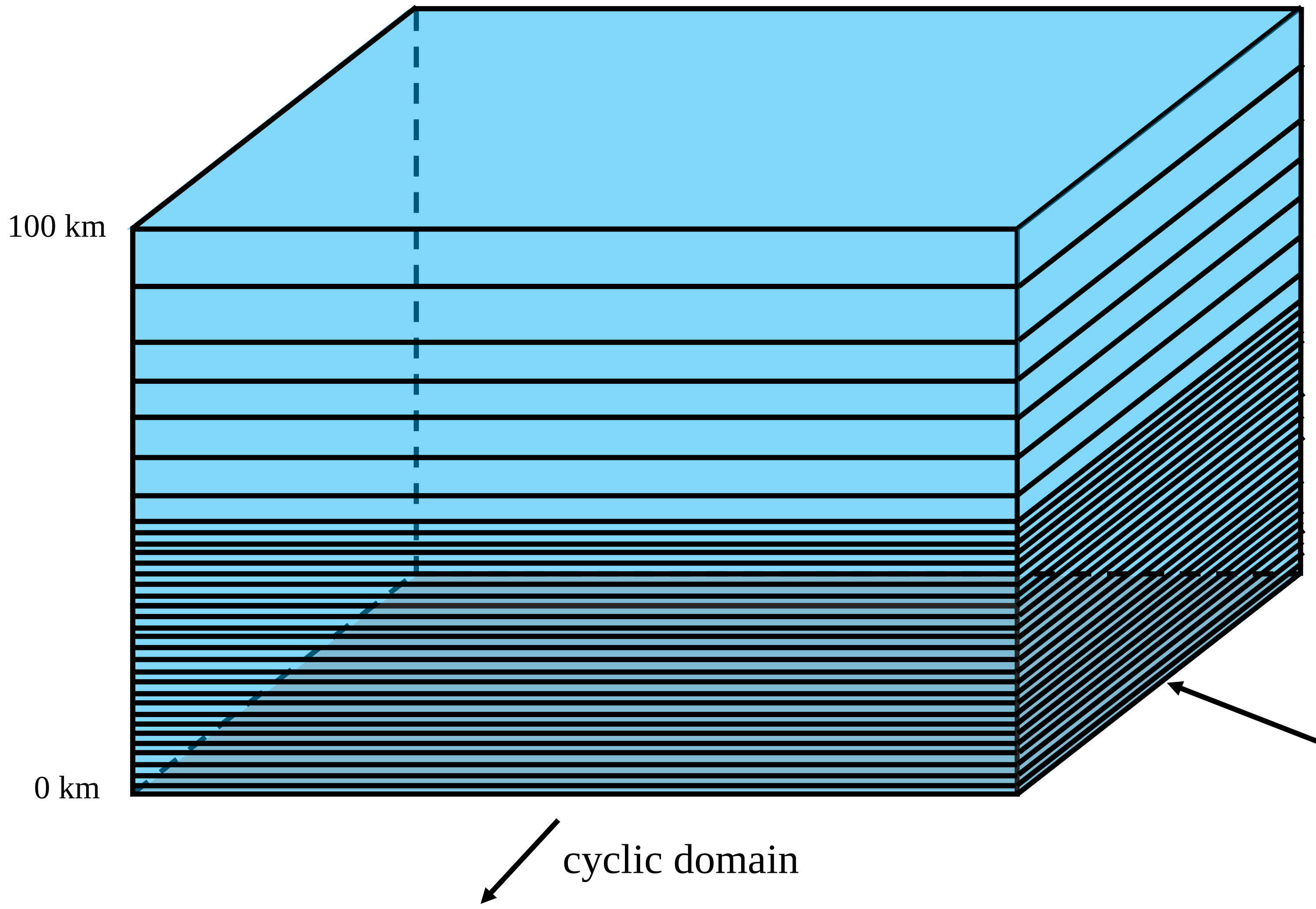

Mid-Latitude Summer (MLS) Profile

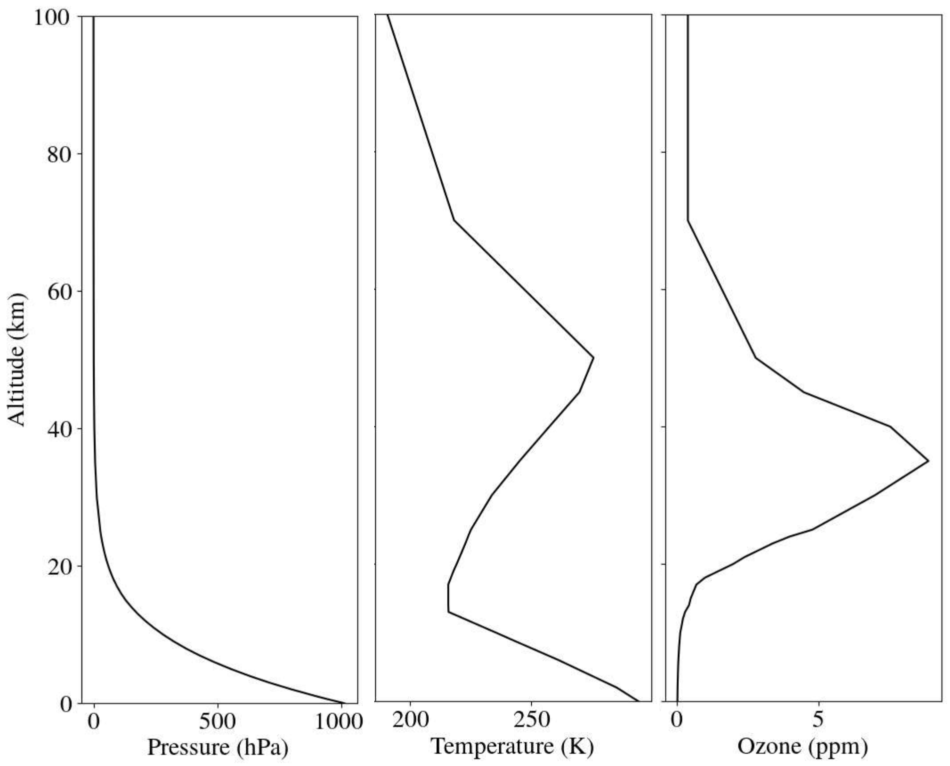

Evaluation of 3D RTM MONKI

Compared with DAK (Doubling Adding KNMI)

De Haan et al, 1987.

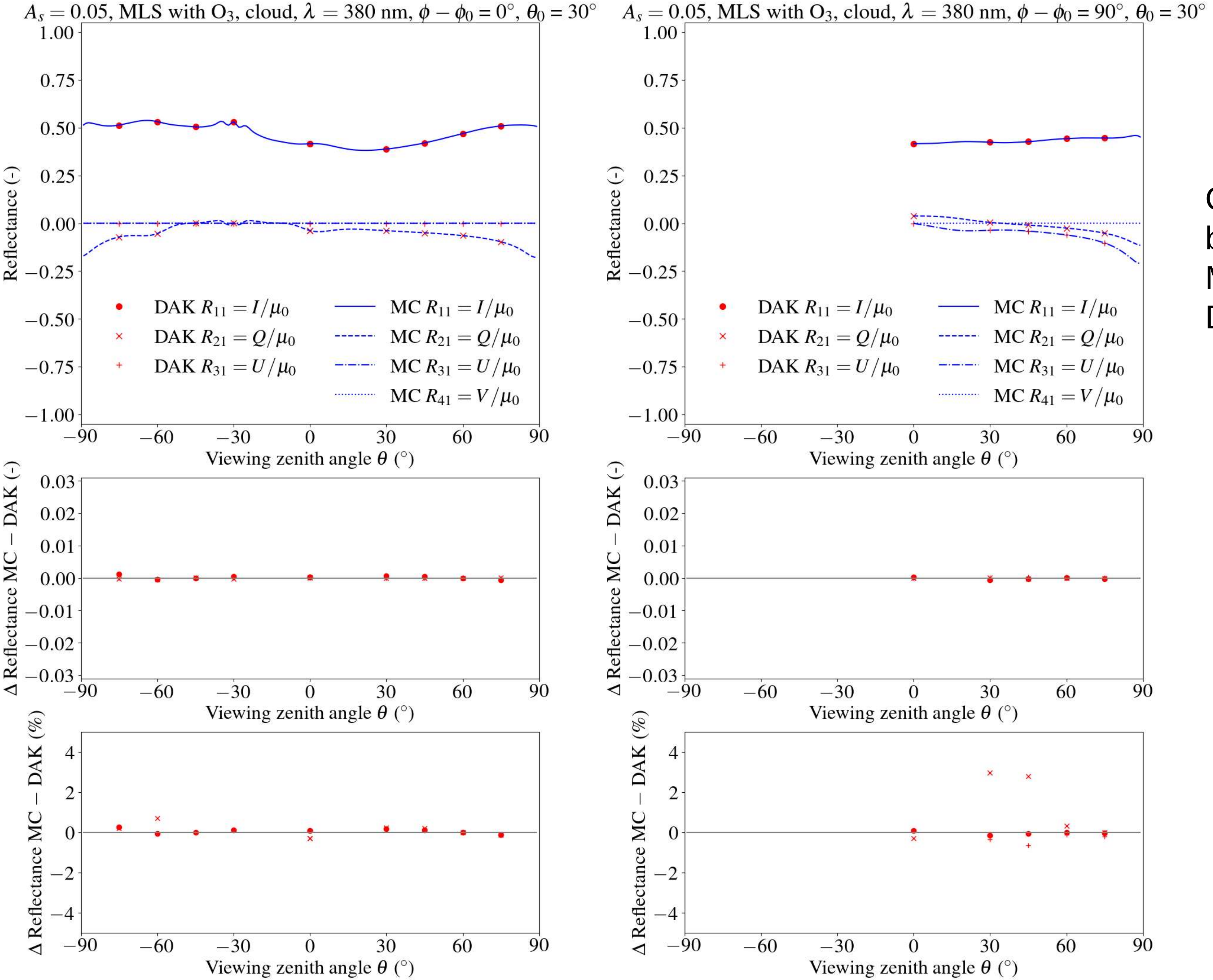

Good agreement between MONKI and DAK

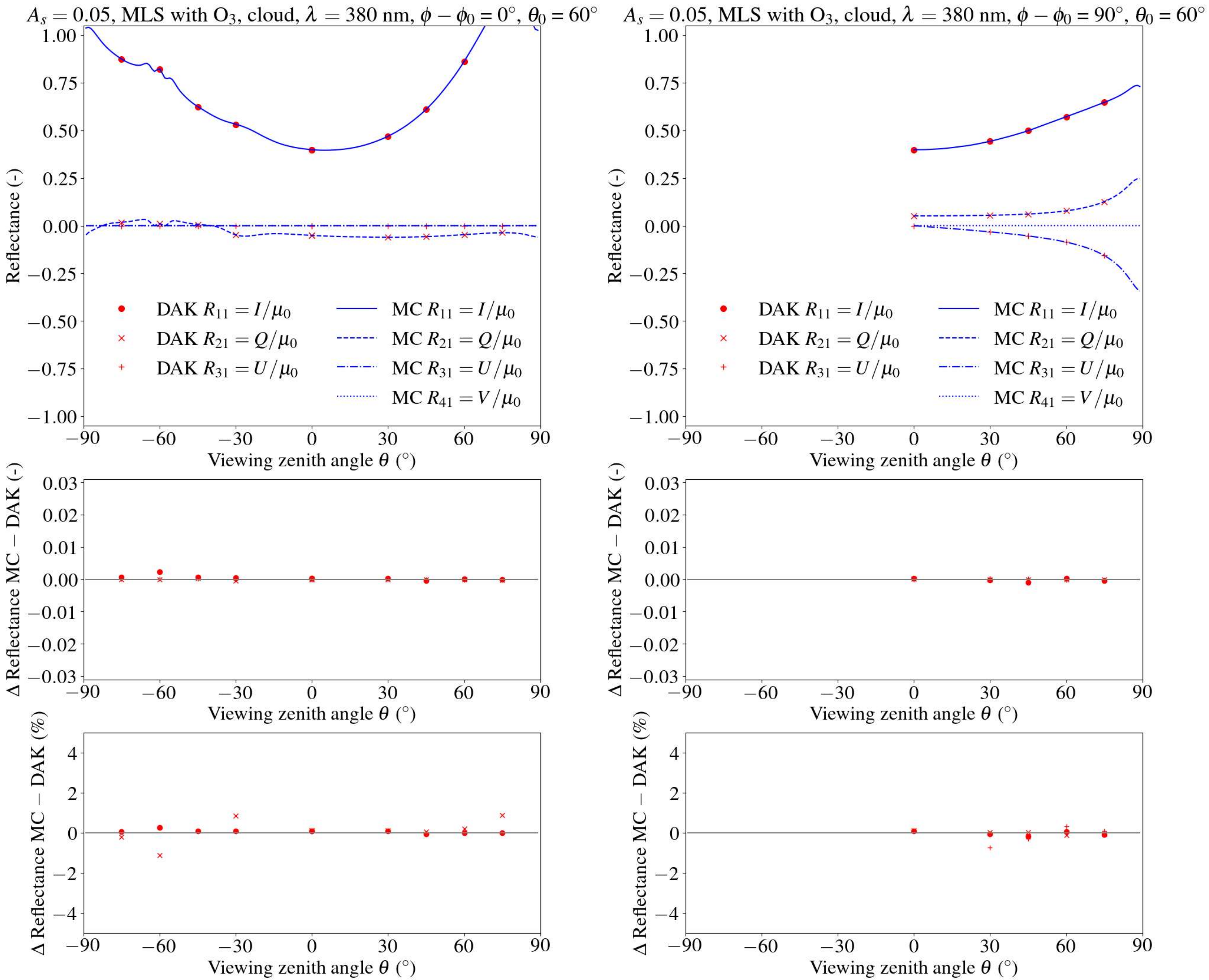

$A_s = 0.05$, MLS with O_3, cloud, $\lambda = 380$ nm, $\phi - \phi_0 = 0°$, $\theta_0 = 60°$
$A_s = 0.05$, MLS with O_3, cloud, $\lambda = 380$ nm, $\phi - \phi_0 = 90°$, $\theta_0 = 60°$
Reflectance (-)
DAK $R_{11} = I/\mu_0$
DAK $R_{21} = Q/\mu_0$
DAK $R_{31} = U/\mu_0$
MC $R_{11} = I/\mu_0$
MC $R_{21} = Q/\mu_0$
MC $R_{31} = U/\mu_0$
MC $R_{41} = V/\mu_0$
Viewing zenith angle θ (°)
Δ Reflectance MC − DAK (-)
Δ Reflectance MC − DAK (%)

MC code setup

- Rayleigh scattering
- O_3 absorption
- Surface reflection
- Mie scattering – clouds

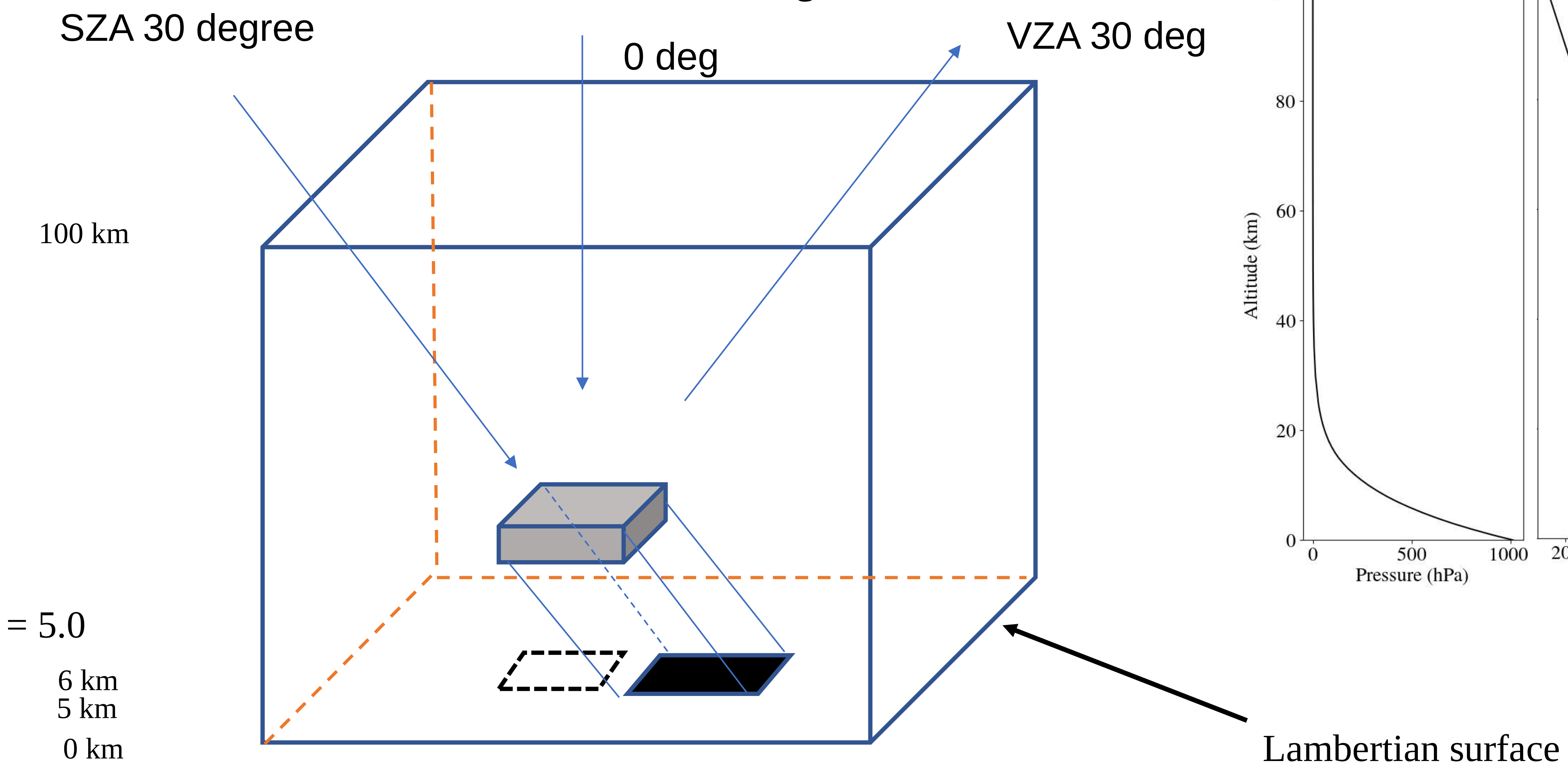

Mid-Latitude Summer (MLS) Profile

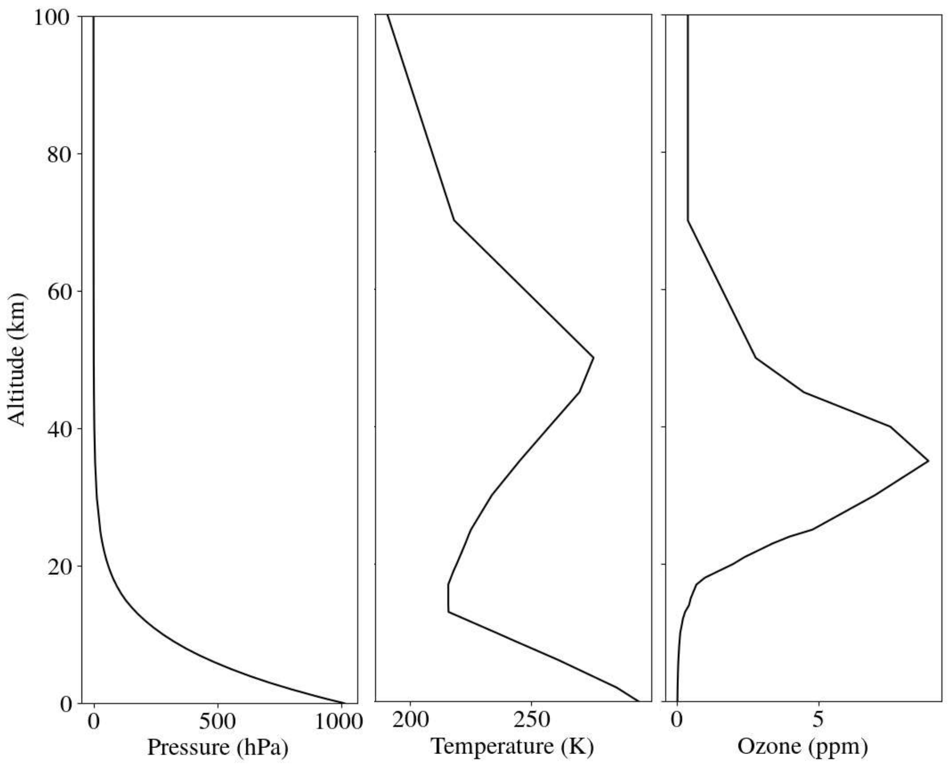

AMF simulated with MONKI

Layer AMF: $$\mathrm{AMF}_i = \frac{\mathrm{SCD}_i}{\mathrm{VCD}_i} = \frac{\int_{\mathrm{path}} c_i \mathrm{d}l}{\int_{z_i}^{z_{i+1}} c_i \mathrm{d}z} = \frac{\int_{\mathrm{path}} \mathrm{d}l}{h_i} = \frac{L_i}{h_i}$$

At 440 nm

Total AMF: $$\mathrm{AMF} = \frac{\sum_l \mathrm{AMF}_l \cdot x_l}{\sum_l x_l}$$

x_l = NO_2 partial column,
NO2 horizontally homogenous in the domain of 200x200 km2

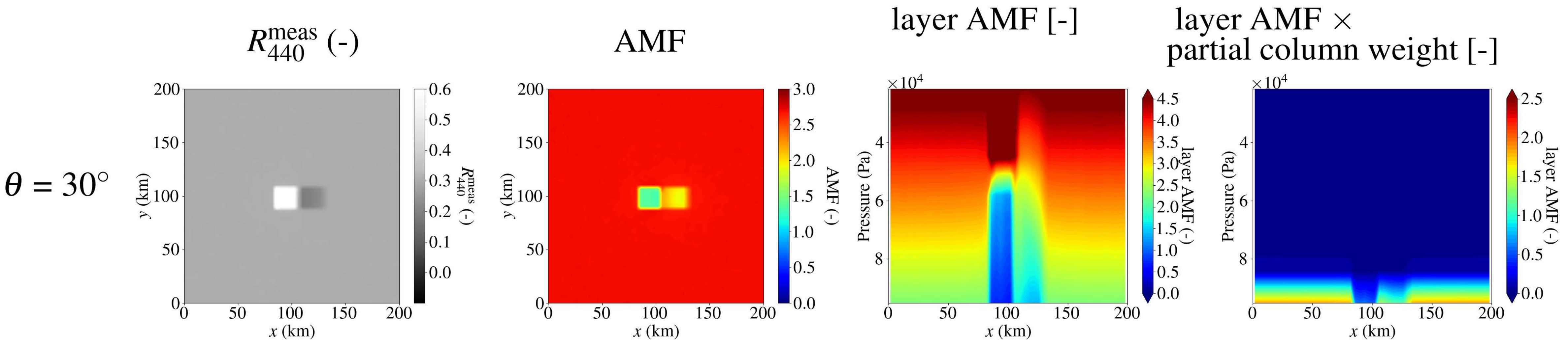

SZA=75 degree, VZA = 30 degree, relative azimuth angle =0, surface albedo = 0.2, COT = 10, cloud at = 5-6 km

AMFs simulated with MONKI at different As

AMF at different surface albedo A_s

$h = 5.0$ km, $\tau_c = 10.0$, $\theta_0 = 75°$, $\phi - \phi_0 = 0°$ $\theta = 60°$

$A_s = 0.0$

$A_s = 0.1$

$A_s = 0.2$

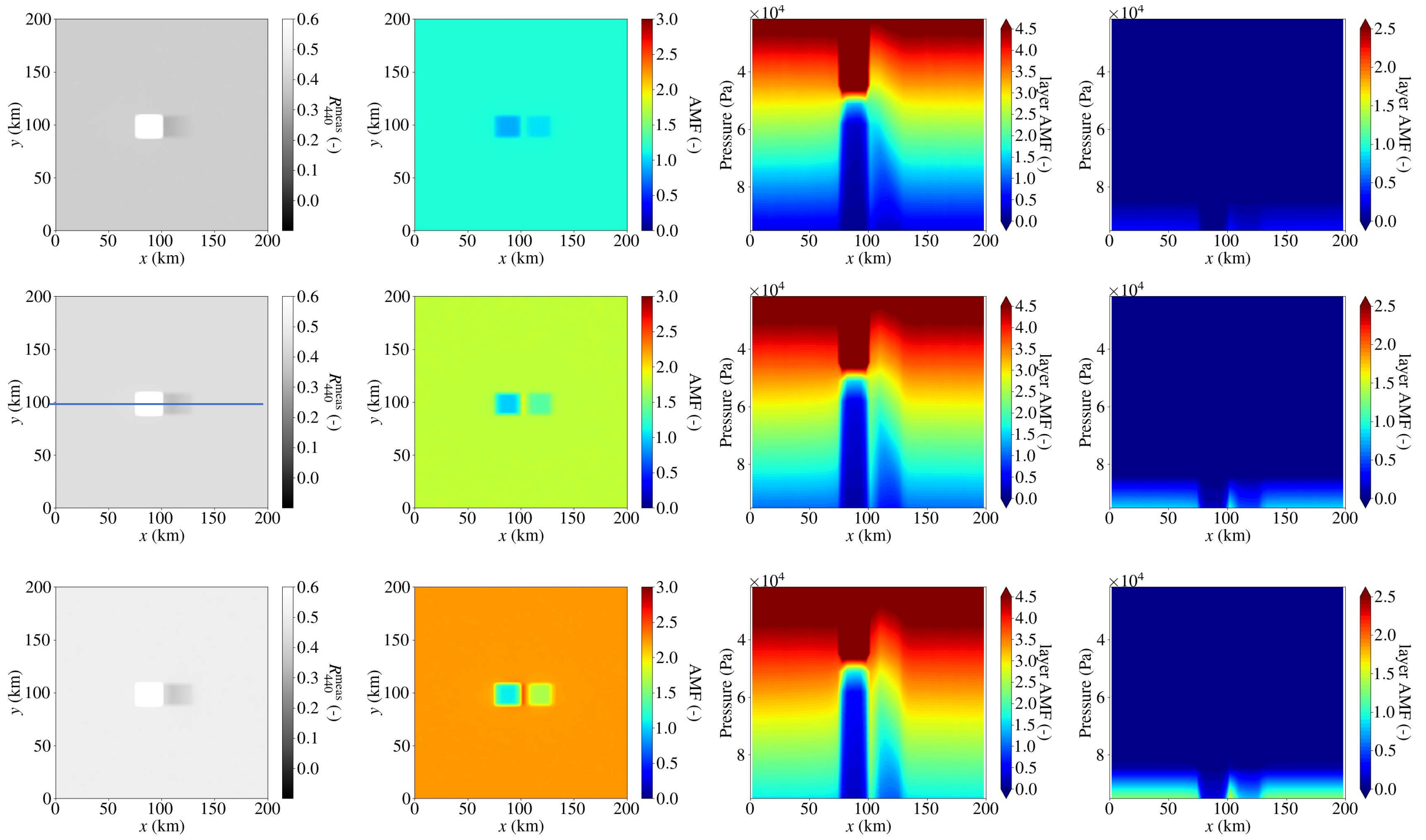

Total AMF

Layer AMF

Layer AMF weighted with NO2 profile

$A_s = 0.2$

AMF at different cloud height h_c

COT=10 $\theta_0 = 75°, \phi - \phi_0 = 0°$ $\theta = 60°$

h_c = 1-2 km

h_c = 5-6 km

h_c = 8-9 km

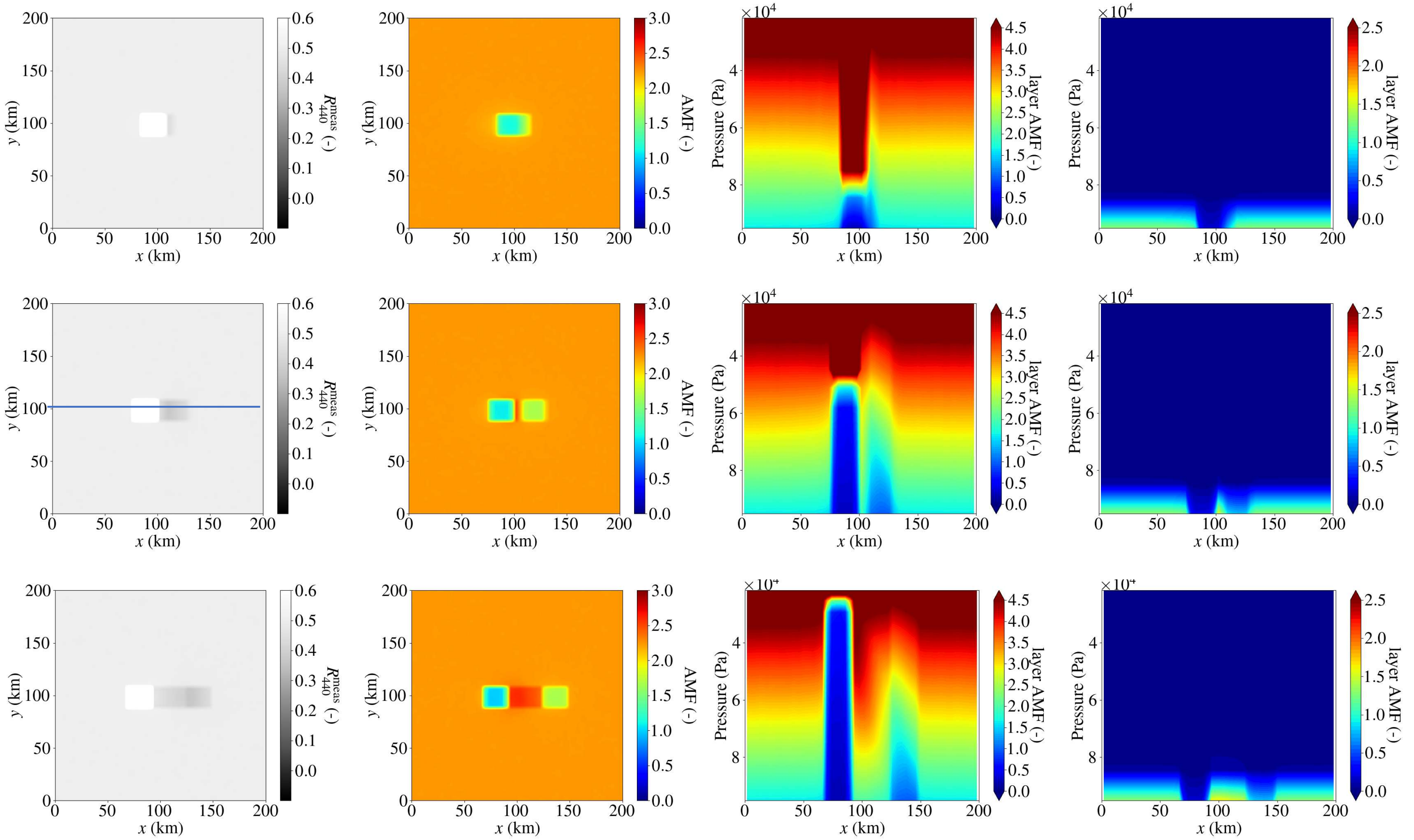

Reflectance at TOA

Total AMF

Layer AMF

Layer AMF weighted with NO2 profile

Total AMF simulated with MONKI, possible explanations

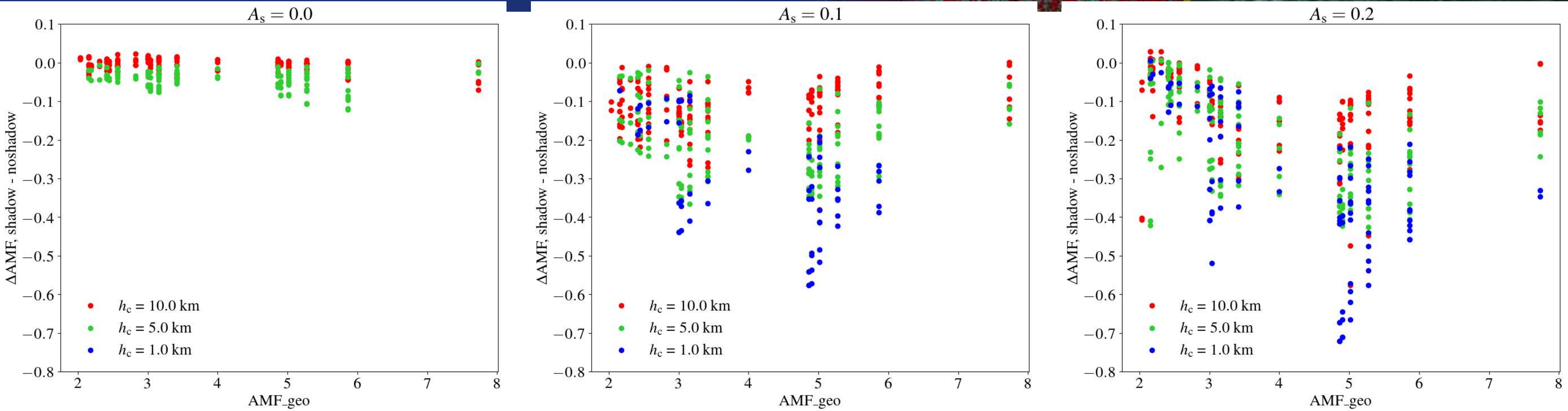

AMF_geo = 1/cos(SZA) + 1/cos(VZA)

Shadow effect in simulated total AMF, while no shadow effect in observed TROPOMI NO_2 VCD?

Simulations used a very high tropospheric NO_2 profile.

Simulation assumed homogeneous NO_2 in the domain.

In real scenes, NO_2 concentration is not as high as in the simulations.

NO_2 natural variation and precision of NO_2 product might mask some shadow effects.

Absorbing Aerosol Index (AAI)

The AAI indicates the presence of UV absorbing aerosols, like desert dust, smoke, volcanic ash.

AAI calculation: compute 340/380 nm reflectance ratio as compared to that of a purely Rayleigh atmosphere

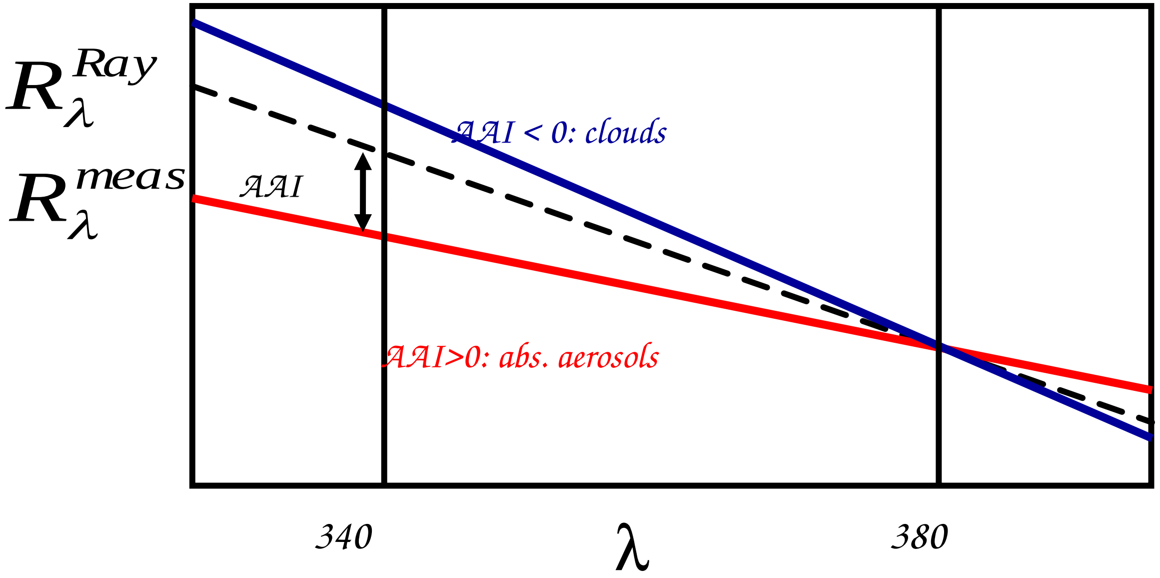

$\mathbf{R}^{meas} = R_{340}/R_{380}$

$\mathbf{R}^{ray} = R^{ray}_{340}/R^{ray}_{380}$ at surface albedo As*

The As* should be calculated so that it produces $R^{ray}_{380} = R_{380}$

$$AAI = -100 \cdot \left[\log_{10}\left(\frac{R_{340}}{R_{380}}\right)^{meas} - \log_{10}\left(\frac{R_{340}}{R_{380}}\right)^{calc} \right]$$

AAI on 31 March 2018

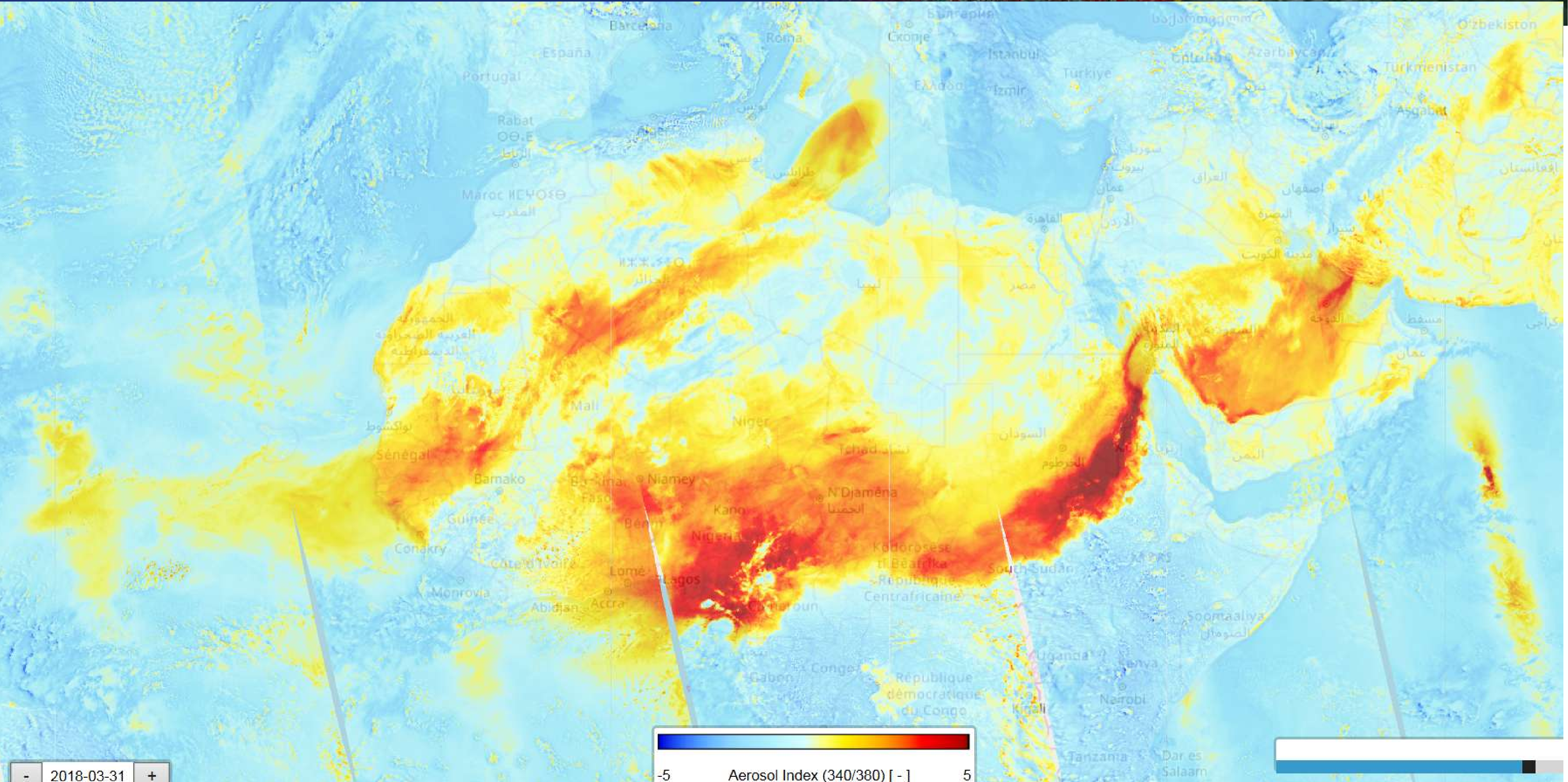

Absorbing aerosol index in cloud shadows

TROPOMI AAI, VIIRS band 07 sun-normalized radiances on 9 October 2018.

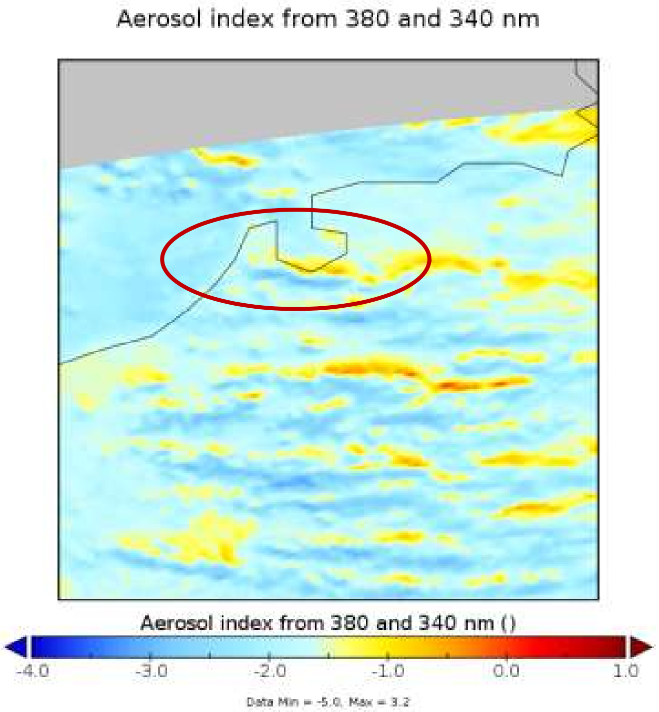

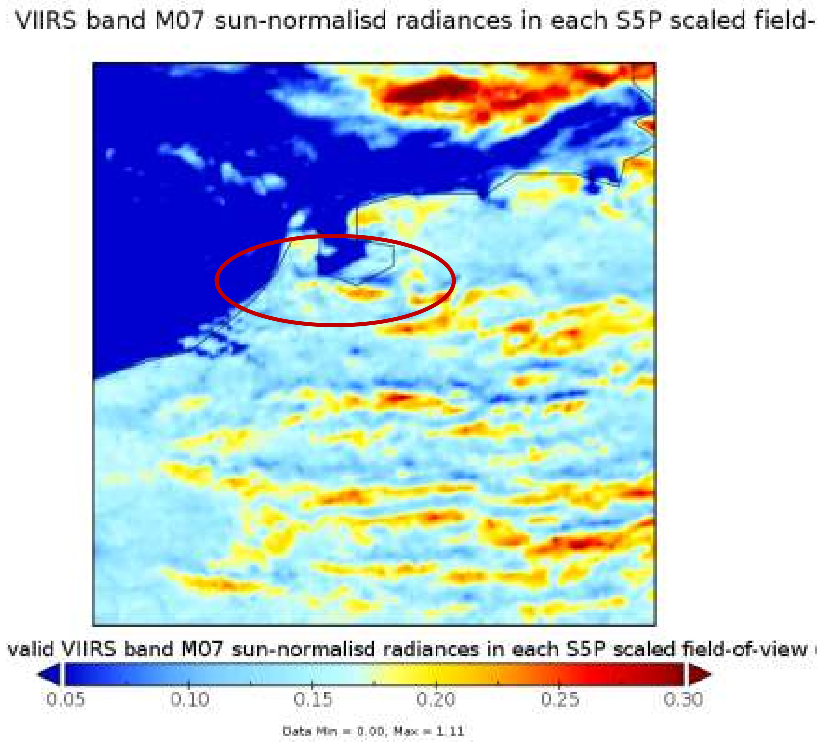

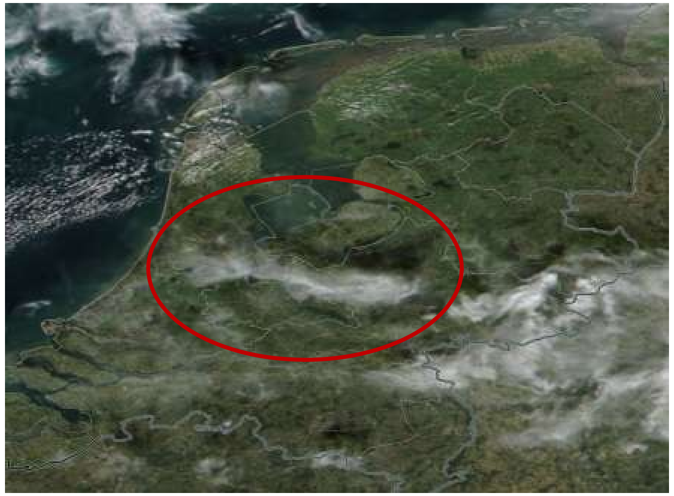

With clouds, no aerosols, AAI is negative.
In cloud shadows, AAI is larger.

COT= 5; cloud extent = 2-3 km (1st row), 5-6 km (2nd row), 8-9 km (3rd row), no aerosols

A_s = 0.1, SZA = 30 deg

Reflectance at 340 nm

Reflectance at 380 nm

A_s = 0.1

A_s = 0.0

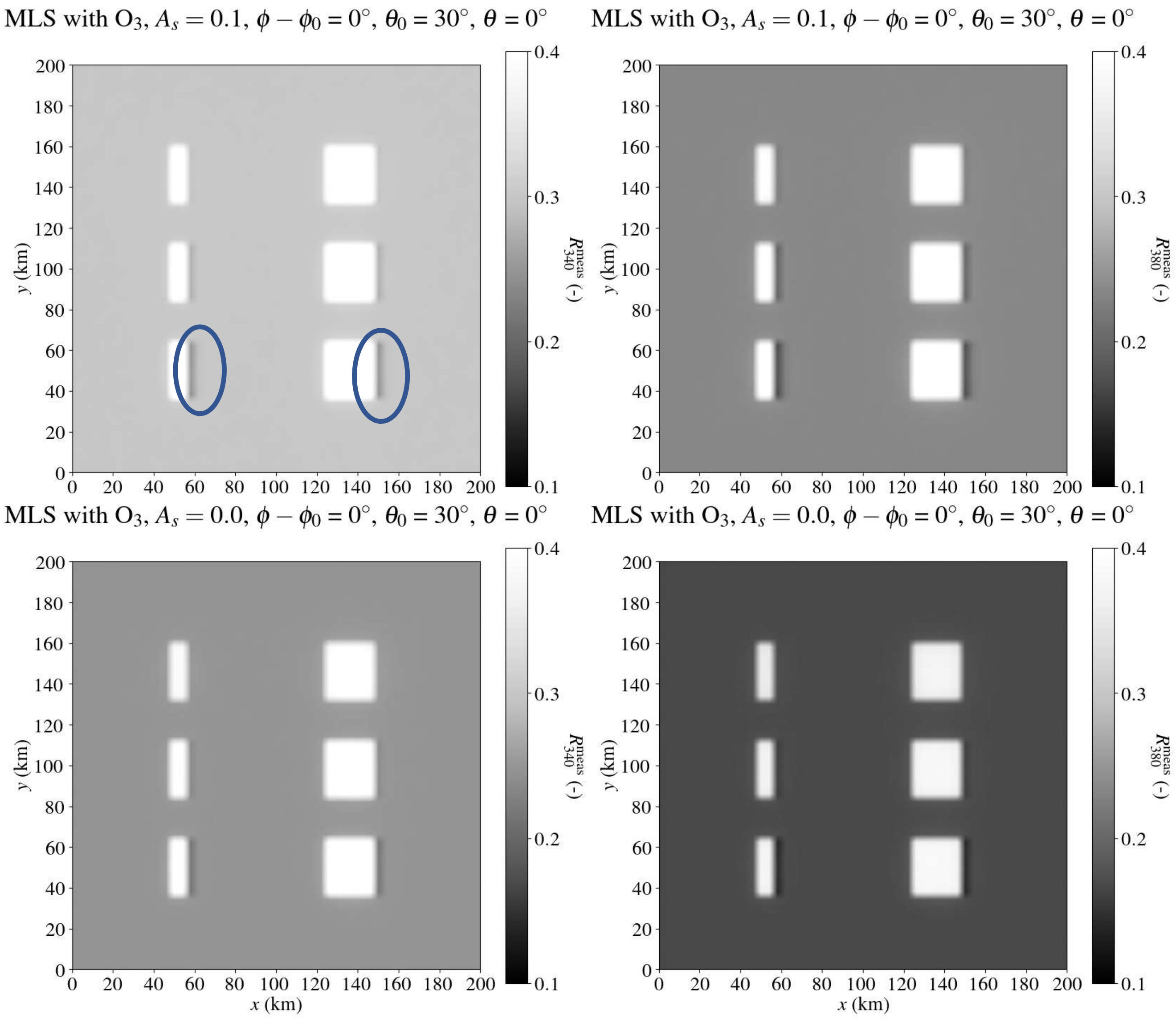

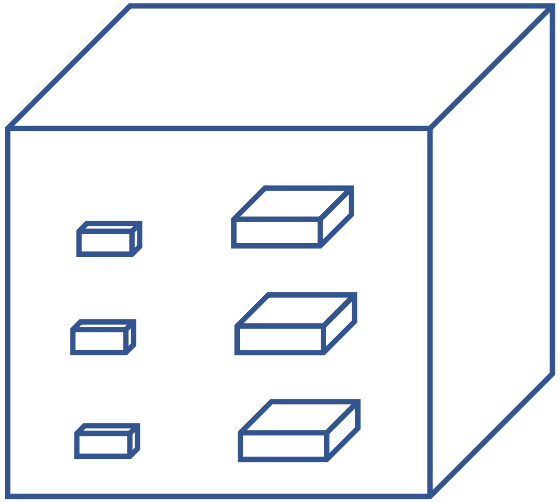

$$AAI = -100 \cdot \left[log_{10}\left(\frac{R_{340}}{R_{380}}\right)^{meas} - log_{10}\left(\frac{R_{340}}{R_{380}}\right)^{calc} \right]$$

A_s = 0.1, SZA = 30 deg
VZA = 0

A_s = 0.1

A_s = 0.0

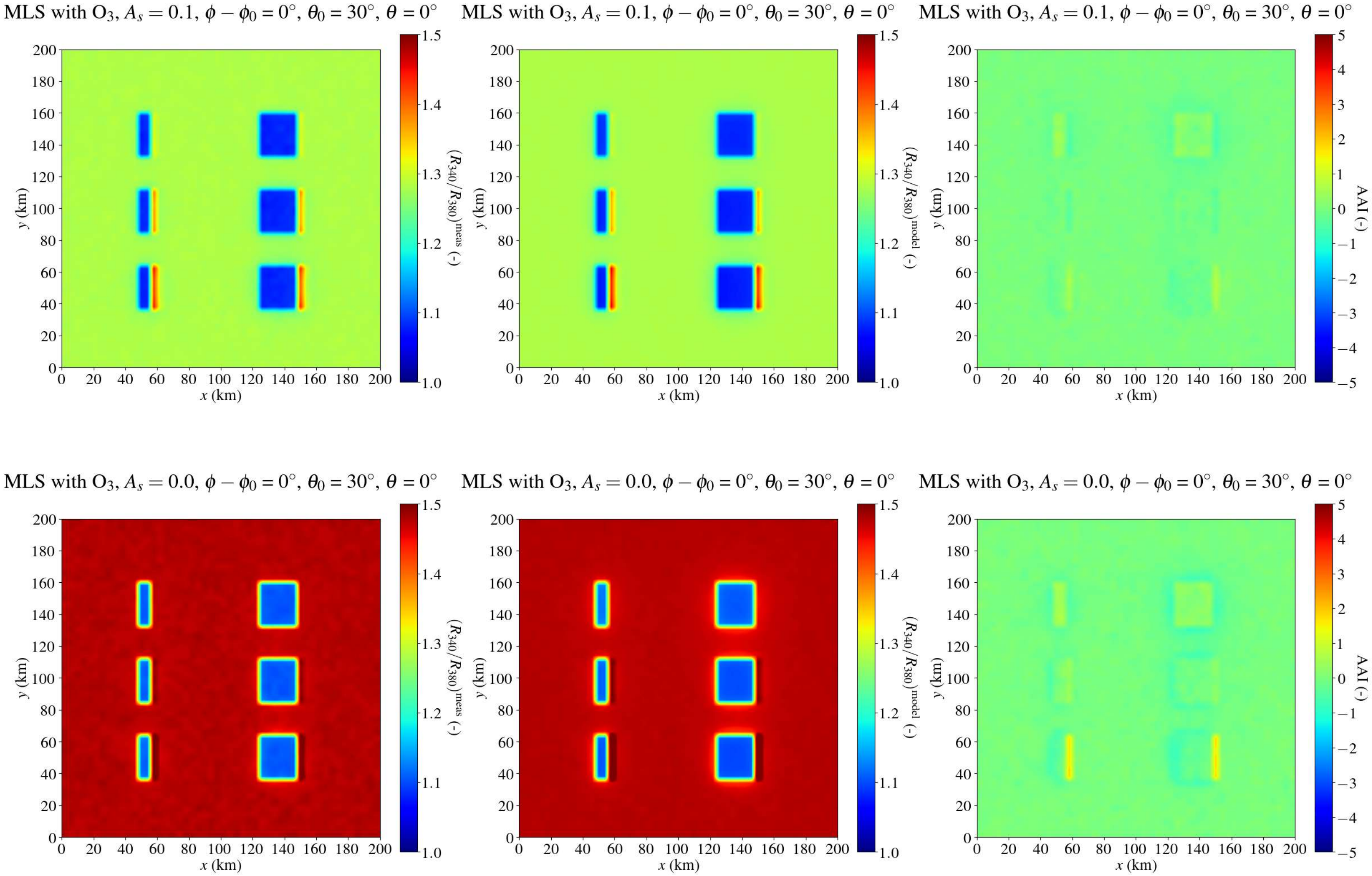

COT= 5;
cloud extent =

2-3 km (1st row),

5-6 km (2nd row),

8-9 km (3rd row)

3D

1D, Rayleigh only, but using As’

AAI

COT= 5; cloud extent = 2-3 km (1st row), 5-6 km (2nd row), 8-9 km (3rd row)

A_s = 0.1, SZA = 30 deg
VZA = 60 deg

A_s = 0.1

A_s = 0.0

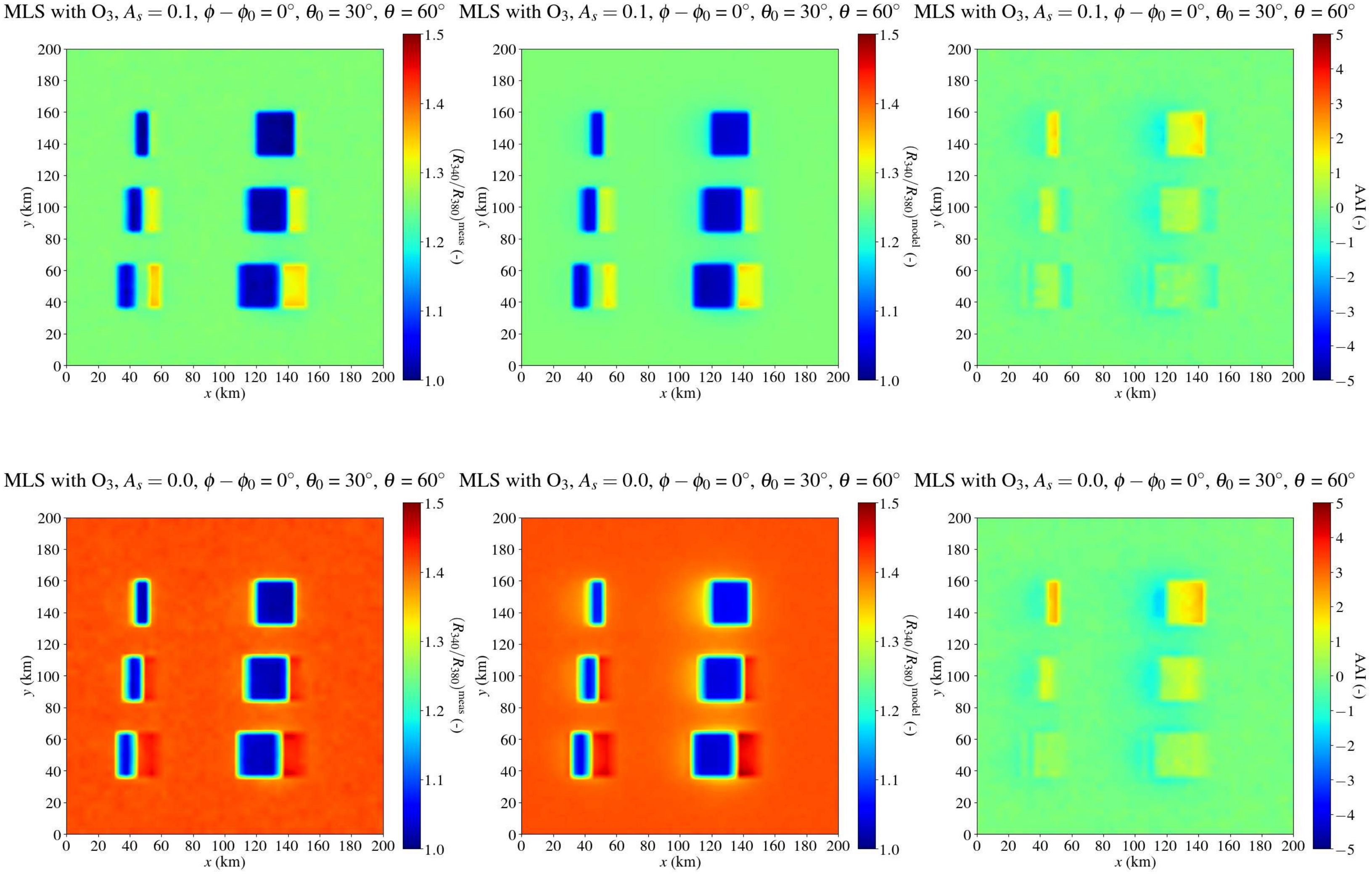

Large VZA, more shadows than nadir view.

3D

1D, Rayleigh only, but using As’

AAI

Cloud shadow effect on Absorbing Aerosol Index: case study Nertherlands/Germany

$$AAI = -100 \cdot \left[log_{10}\left(\frac{R_{340}}{R_{380}}\right)^{meas} - log_{10}\left(\frac{R_{340}}{R_{380}}\right)^{calc} \right]$$

TROPOMI observations:

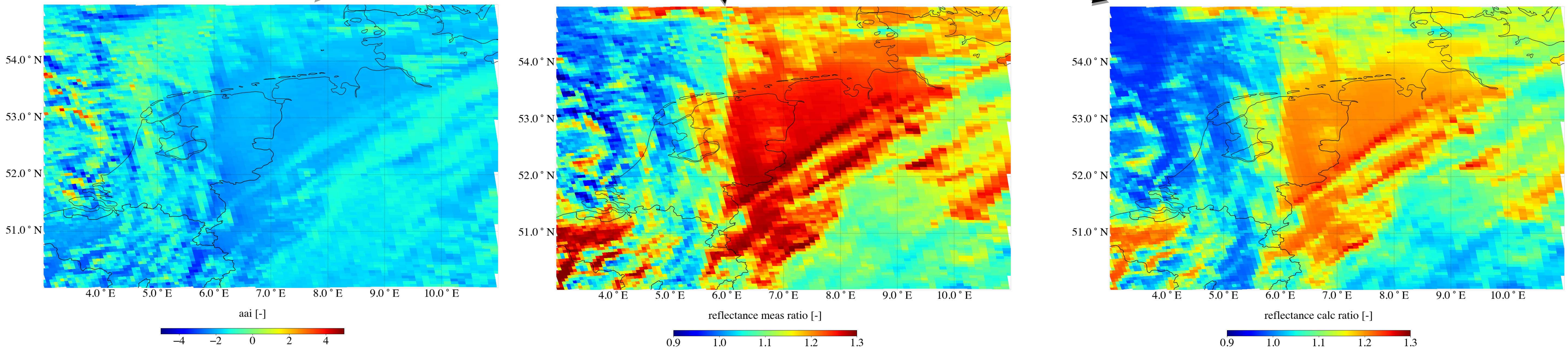

MONKI simulations:

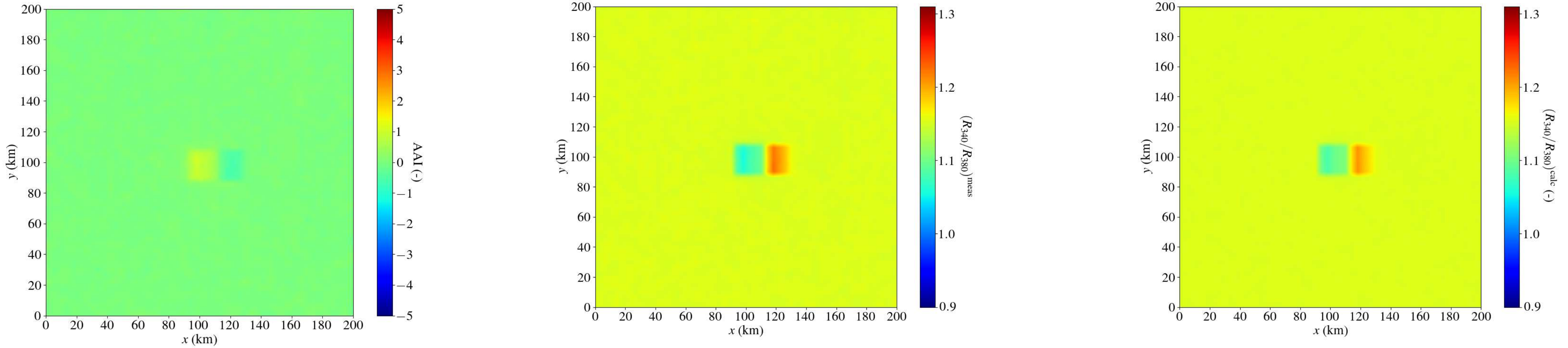

Results: AOD retrievals using shadows: principle

- Reflectance for a shadow pixel

$$I_s = I_{path} + \frac{t_{dif}(\mu_0)\,T(\mu_v)\,A}{(1-AS)}$$

- Reflectance for a bright pixel

$$I_b = I_{path} + \frac{\left(e^{-\tau/\mu_0} + t_{dif}(\mu_0)\right)T(\mu_v)\,A}{(1-AS)}$$

- Assume same surface albedo at the two pixels

$$\frac{I_b - I_{path}}{I_s - I_{path}} = \frac{e^{-\tau/\mu_0} + t_{dif}(\mu_0)}{t_{dif}(\mu_0)}$$

- Minimize the difference to get AOD

$$\varepsilon = \left| \frac{I_b - I_{path}}{I_s - I_{path}} - \frac{e^{-(\tau_r+\tau_a)/\mu_0} + T_{dif}(\mu_o)}{T_{dif}(\mu_o)} \right|$$

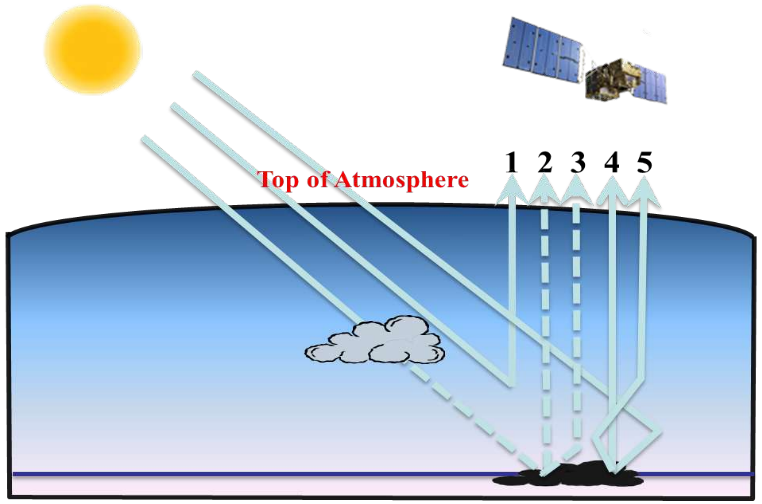

Duan , 2001

1 atmospheric path

2,4 surface reflection

3,5 inter-action between surface and atmosphere

Results: aerosol retrievals using cloud shadows: Landsat-8 data

OLI / Landsat 8, 11 Feb.,2013

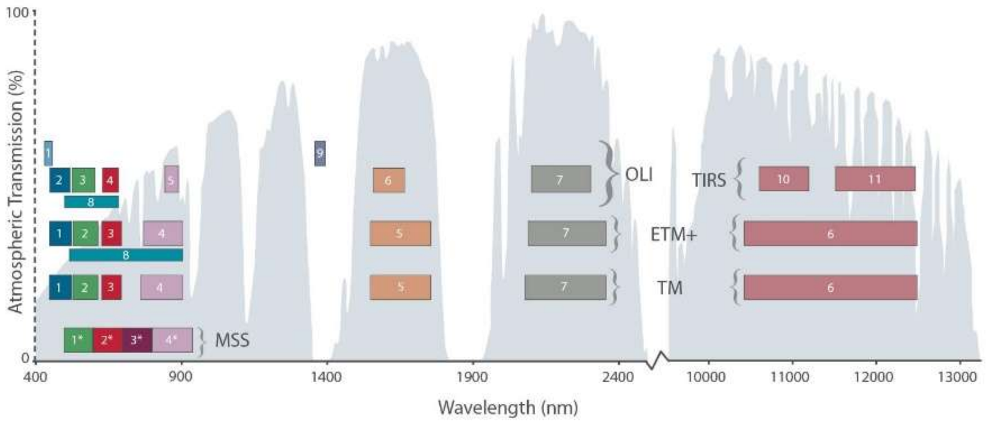

* MSS bands 1–4 were known as bands 4–7, respectively, on Landsats 1–3

Band	Wavelength (um)	Spatial Resolution (m)
B01	0.43 ~ 0.45	30
B02	0.45 ~ 0.51	30
B03	0.53 ~ 0.59	30
B04	0.64 ~ 0.67	30
B05	0.85 ~ 0.88	30
B06	1.57 ~ 1.65	30
B07	2.11 ~ 2.29	30
B08	0.50 ~ 0.68	15
B09	1.36 ~ 1.38	30
B10	10.60 ~ 11.19	100
B11	11.50 ~ 12.51	100

Screening and selection of cloud shadows

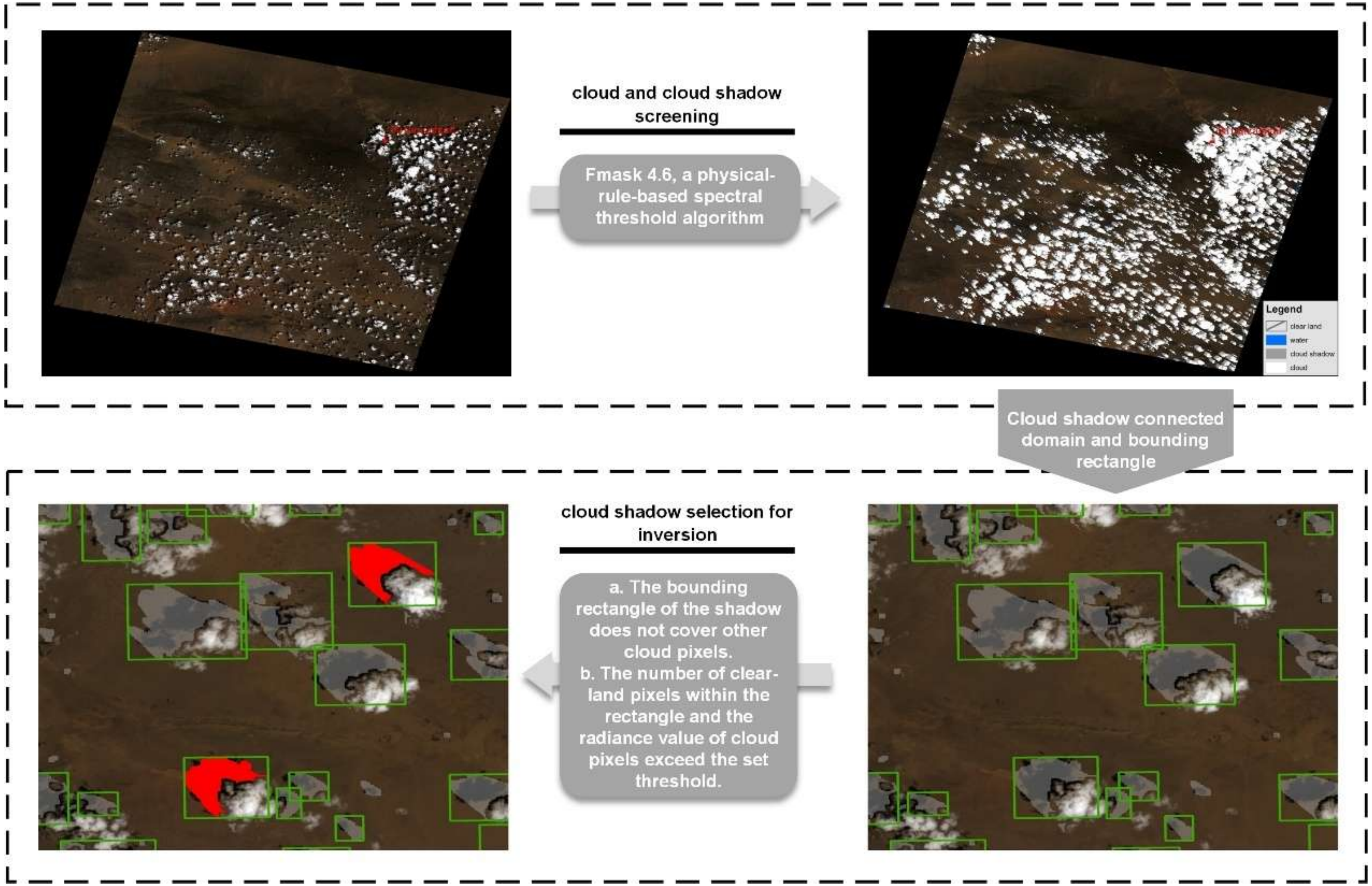

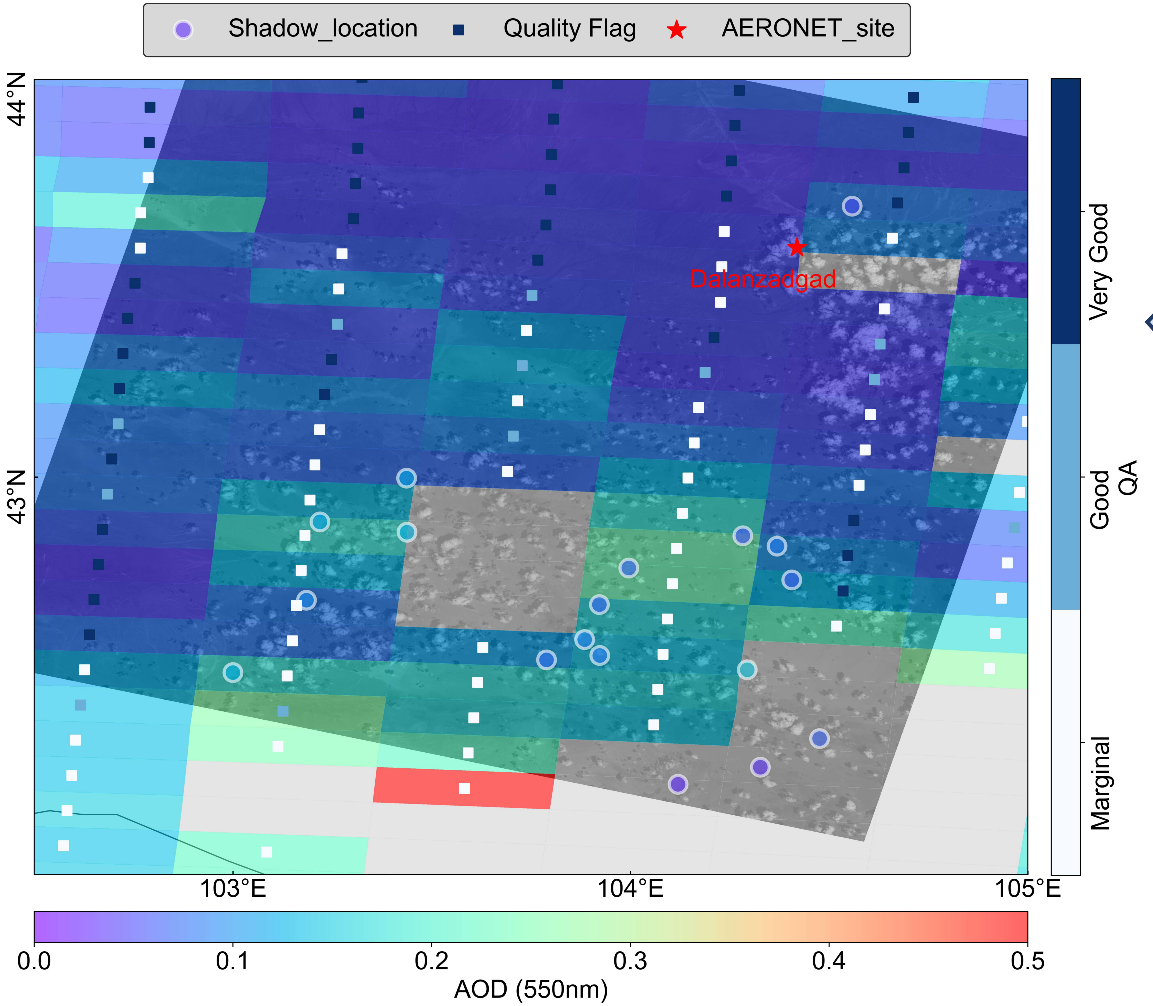

Figure1. The AOD (550 nm) distribution map provided by the MODIS aerosol product, the base map is the LANDSAT8 image on June 23, 2017, the squares in the grid represent the QA of the AOD retrievals, and the dots represent the AOD retrieved by the cloud shadow.

- The conventional aerosol satellite retrieval algorithms in cloudy areas find it challenging to provide relatively accurate AOD.
- The cloud shadow method can effectively enhance the efficiency of AOD retrieval in cloudy regions.

Results

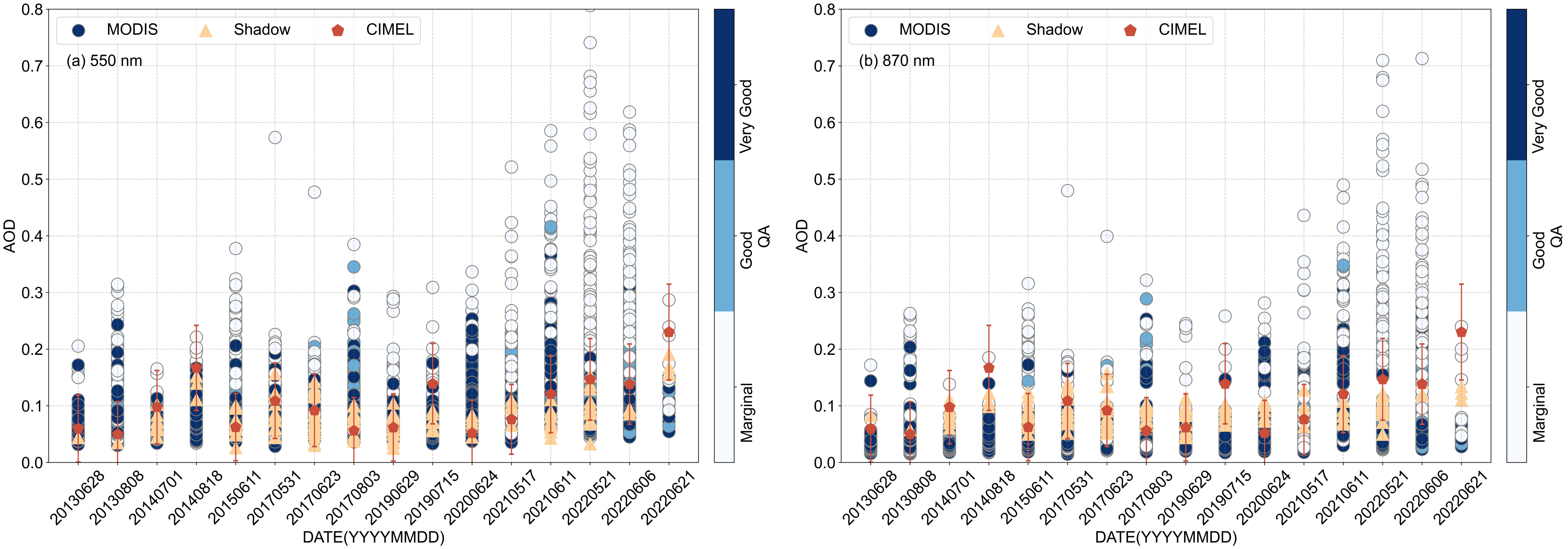

Figure2. The AOD obtained by cloud shadow algorithm inversion on 16 remote sensing images, MODIS aerosol products and AERONET site data.

- The AOD obtained by the cloud shadow algorithm is very close to the ground-based sun photometer data, and the deviations are basically within ±0.05.

European Young scientists contributions in Dragon 5

Name	Institution	Poster title	Contribution including period of research
Benjamin Leune	KNMI	Observing and Simulating 3D Cloud Effects in the S5P NO2 Product	Analyzed the 3D model simulated NO2 observations and TROPOMI NO2 data for cloud effects.
Victor Trees	KNMI/TU-Delft		Developed MONKI 3D radiative transfer model, simulated AAI and NO2 measurements from TROPOMI with the 3D model. Analyzed the simulated AAI and NO2 observations
			Submitted manuscript about clouds disappearing during eclipse.

Chinese Young scientists contributions in Dragon 5

Name	Institution	Poster title	Contribution including period of research
Congcong Qiao	IAP	A New Algorithm for Deriving Aerosol Optical Depth Over Cities Using the Building Shadows of High-resolution Satellite Imagery	Aerosol optical thickness retrievals from GF-2 and Landsat-8
			Submitted manuscript to GRL about deriving AOD over cities using the building shadows

Plans for year 4

- Publish the AOD retrieval paper using GF-2 and Landsat-8 scenes (submitted)
- Apply automatic shadow detection algorithm on GF-2 and Landsat-8

- Finalize and publish the analysis of clouds shadows in S5P NO2 products (in preparation)
- Finalize and publish the analysis of clouds shadows in S5P AAI products (in preparation)
- Improve NO2 retrievals at high spatial resolution (to be done)

Publications

Qiao, C., Liu, S., Huo, J., Mu, X., Wang, P., Jia, S., Fan, X., and Duan, M.: Retrievals of Precipitable Water Vapor and Aerosol Optical Depth from direct sun measurements with EKO MS711 and MS712 Spectroradiometers, , Atmos. Meas. Tech., 2022.

Qiao et al., A Novel Algorithm for Deriving Aerosol Optical Depth over Cities Using the Building Shadows of High-resolution Satellite Imagery, submitted to GRL, 2023.

Trees, V., Wang, P., and Stammes, P.: Restoring the top-of-atmosphere reflectance during solar eclipses: a proof of concept with the UV Absorbing Aerosol Index measured by TROPOMI, Atmos. Chem. Phys., 21, 8593–8614, https://doi.org/10.5194/acp-21-8593-2021, 2021.

Trees, V. J. H., Wang, P., Stammes, P., Tilstra, L. G., Donovan, D. P., and Siebesma, A. P.: DARCLOS: a cloud shadow detection algorithm for TROPOMI, Atmos. Meas. Tech., 15, 3121–3140, https://doi.org/10.5194/amt-15-3121-2022, 2022.

Trees et al., Rapid cloud dissipation during solar eclipses due to land surface cooling, in review in nature Communications Earth & Environment, 2023.